

# Protein–Membrane Interaction Probed by Single Plasmonic Nanoparticles

Cristina L. Baciú,<sup>†</sup> Jan Becker,<sup>†</sup> Andreas Janshoff,\* and Carsten Sönnichsen\*

*Institute of Physical Chemistry, University of Mainz, Jakob-Welder-Weg 11, 55128 Mainz, Germany*

Received March 20, 2008; Revised Manuscript Received April 16, 2008

## ABSTRACT

We present a nanosized and addressable sensor platform based on membrane coated plasmonic particles and show unequivocally the covering with lipid bilayers as well as the subsequent detection of streptavidin binding to biotinylated lipids. The binding is detected on membrane covered gold nanorods by monitoring the spectral shift by fast single particle spectroscopy (fastSPS) on many particles in parallel. Our approach allows for local analysis of protein interaction with biological membranes as a function of the lateral composition of phase separated membranes.

The detection of noncovalent binding events is a fundamental goal of contemporary analytical chemistry, for example, in high throughput screening (HTS) of drug candidates from large libraries of molecules that potentially recognize a specific surface receptor. HTS heavily relies on sophisticated strategies to miniaturize the devices, in particular, the sensing area. However, miniaturization is ultimately limited by the increasing stochastic noise emitted by the small area, which eventually exceeds the actual sensor signal. This small-area regime, however, renders conventional analysis of surface binding cumbersome because of decreasing signal-to-noise ratios. Often overlooked is the fact that the noise produced in small systems comprises valuable information about all involved rate constants as produced by equilibrium coverage fluctuations.<sup>1</sup> It is in principle possible to extract relevant kinetic parameters from a system that is inherently in equilibrium without interference with mass transport as often faced in diluted systems. Small sensing areas are required to exploit the noise generated by coverage fluctuations and this work deals with the necessary requirements of the next generation of stochastic sensing on surfaces. Single gold nanoparticles can be used as sensors for their local environment by detecting the plasmon shift induced by changes in the refractive index.<sup>2–5</sup> Motivation for single particle based detection of membrane protein interaction is also provided by contemporary research on the lateral organization of biological membranes.<sup>6</sup> Particularly, elucidation of occurrence and function of nanodomains (also termed rafts) that are required for general membrane function are challenging targets for the proposed detection scheme based on mem-

brane coated particles.<sup>7</sup> Employing particles as nanoscopic reporters for biomolecular interactions on the level of few (<50) proteins offers the possibility to screen lateral inhomogeneities of native membranes.

Proper functionalization remains an issue if it comes to real world applications, in particular, biological relevant samples such as membrane associated proteins and peptides. In this context, membrane mimics are an attractive solution to achieve an almost native environment with high surface coverage and miniscule nonspecific adsorption. Solid supported membranes are among the most versatile sensing platforms to study both molecular recognition events usually taking place at cellular membranes and ionic transport across bilayers.<sup>8</sup> A large variety of different model systems have been successfully established, and the approaches include simple self-assembled lipid bilayers on various supports such as glass, metal electrodes, or semiconductors.<sup>9</sup> Lately, more advanced systems were created employing porous supports or using tethered lipids that allow functional insertion of membrane proteins.<sup>10</sup> Only few studies report on particles successfully covered with lipid bilayers.<sup>11,12</sup> This is mostly because parameters such as membrane curvature and adhesion properties need to be carefully adjusted.

We created a sensor platform based on individual gold nanorods immobilized randomly on a solid support and covered entirely with a fluid membrane displaying biotin moieties (Figure 1). The fluorescently labeled (BodiPY-PC) membrane is formed by vesicle spreading in microcapillaries.<sup>13</sup> The homogeneous green fluorescence from the membrane, visible directly under white light dark-field illumination, shows successful spreading of a closed lipid bilayer (Figure 1b). The gold nanorods appear as brightly colored spots under dark-field illumination due to the excitation of

\* Corresponding authors. E-mail: Janshoff@uni-mainz.de (A.J.) and Soennichsen@uni-mainz.de (C.S.).

<sup>†</sup> Contributed equally and in alphabetical order.

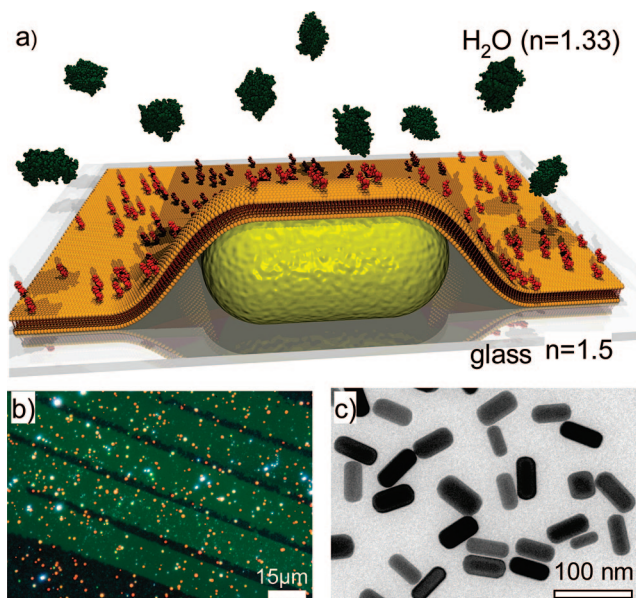


**Figure 1.** (a) Schematics of a gold nanorod (yellow) coated with a partly biotinylated (red) membrane (orange) and exposed to streptavidin (green). The scheme presents the ideal case of a complete membrane coverage without any defects. The glass support has a refractive index of  $n = 1.5$ ; the aqueous buffer has a refractive index of  $n = 1.33$ . (b) Darkfield image of gold nanorods (bright spots) covered by a lipid membrane (greenish background) is structured on this substrate by a micro-molding in capillaries.<sup>20</sup> (c) Transmission electron microscope (TEM) image of gold nanorods used in this work (mean length  $56 \pm 5$  nm, width  $26 \pm 5$  nm, aspect ratio  $2.2 \pm 0.4$  nm, determined from 100 particles).

plasmons at their specific plasmon resonance wavelength. Fluorescence recovery after photobleaching (FRAP) confirms that lateral mobility of the supported membrane is preserved (Supporting Information, Figure S1). The diffusion coefficients determined by FRAP are in the range of  $4\text{--}5 \mu\text{m}^2/\text{s}$ , similar to the control experiments in the absence of gold nanoparticles ( $5 \pm 1 \mu\text{m}^2/\text{s}$ ) and those reported earlier for this case.<sup>14</sup> Some fraction (2–10 mol %) of the lipids in the membrane is labeled with biotinylated lipids (Biotin-DHPE and Biotin-X-DHPE; see Supporting Information), sufficient to produce a complete streptavidin monolayer on top of the membrane. Streptavidin binding was confirmed by ellipsometry measurements revealing an additional height increase of 2.34 nm for the Biotin-DHPE and 3.12 nm for the Biotin-X-DHPE membrane. This thickness is additional to the 3.95 nm height increase due to spreading of the membrane (Supporting Information, Figure S2).

The gold nanorods we used were synthesized using the procedure published by Nikoobakht et al.<sup>15</sup> In this two-step synthesis, preformed seeds grow into rods in a concentrated surfactant solution. The gold nanorods used in this work had mean lengths of  $56 \pm 5$  nm, mean widths of  $26 \pm 5$  nm, and mean aspect ratios of  $2.2 \pm 0.4$  nm as determined from measuring 100 particles on TEM images like that in Figure 1c.

We are able to detect streptavidin binding to several membrane coated particles in parallel using a fast single particle spectroscopy (fastSPS) method based on an elec-

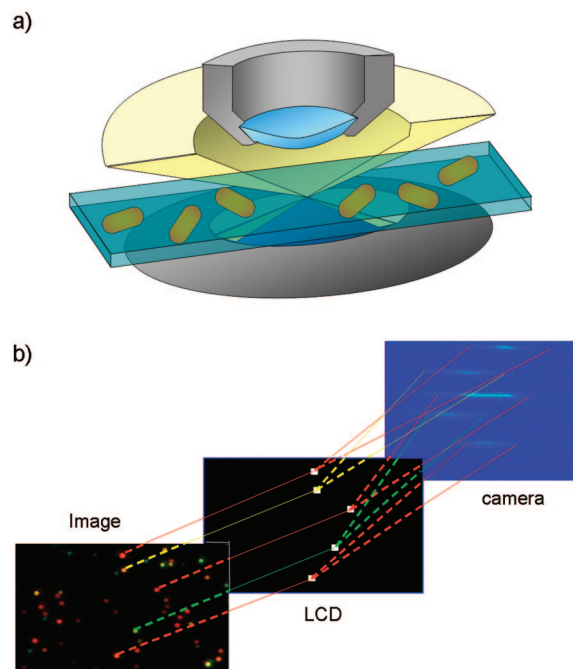


**Figure 2.** (a) Schematics of the dark-field microscope setup. The scattered light is directed either to the ocular or to an imaging spectrometer, where the light is dispersed and the resulting spectrum captured by a CCD camera. (b) In the fastSPS method, the entrance slit of the spectrometer is replaced by an electronically addressable liquid crystal device (LCD) placed in the microscope's image plane. Each of the LCD pixels acts as an electronically addressable shutter for a small area of the sample. We set LCD pixels corresponding to vertically separated particles to transparent in order to spectrally investigate those particles simultaneously.<sup>16</sup>

tronically addressable shutter.<sup>16</sup> To optically observe single particles, we use a standard transmission type dark-field microscope coupled to an imaging spectrometer and a 100 W tungsten lamp as light source (Figure 2a).<sup>17</sup> We have replaced the entrance slit of the spectrometer by an electronically addressable liquid crystal device [LCD; LC2002, Holoeye;  $800 \times 600$  pixels ( $230 \times 230$  pixels used in our setup) with  $(32 \mu\text{m})^2$  pixel size] so that each of its pixels acts as an individual electronically addressable shutter. By setting an LCD pixel to transparent, a corresponding particle is spectrally investigated (Figure 2b). This setup allows the simultaneous spectral investigation of up to 20 vertically separated particles before overlap between spectra becomes problematic. All spectra are background corrected, normalized to the spectral characteristic of the setup, and smoothed over 5 points (4 nm). The maximum of the plasmon resonance is determined by a parabolic fit around the absolute maximum, and every particle was investigated five times at each step of the experiment. Singular outliers (more than 6 nm difference from mean) resulting from light scattered by small dust particles flowing by are not considered when averaging. The spectral position of the rods is determined with a reproducibility of less than 1 nm.

To immobilize gold rods on a glass substrate, we dilute the as prepared rod–solution 1:10 with distilled water and rinse them for 5 min through a flow-cell consisting of a thin, flat glass capillary ( $0.1 \text{ mm} \times 2 \text{ mm} \times 100 \text{ mm}$ ) connected

to PET tubing. Some of the rods stick to the glass surface, which is enhanced by the addition of a small amount of sodium chloride. When enough rods are immobilized in the field of view, we rinse with distilled water for 30 min to remove unbound rods and surfactant from the growth-solution. Subsequently, the sample is rinsed with PBS buffer for an additional 5 min to ensure that the gold particles are in the same environment in all of the following measurements. At this point, we record the spectra of 29 particles in the field of view. Each particle is investigated five times to get statistics and enhance the accuracy of the mean. Figure 3a shows a typical example of such a single particle spectrum.

Now, we flush in lipid vesicles and incubate for 30 min in order to spread a membrane bilayer on the substrate. Subsequent washing with PBS buffer for 60 min removes excess lipid vesicles. BodiPy-fluorescence from markers in the lipids (1 mol %) is used to ensure that the glass surface in the field of view is indeed covered by a membrane. The illumination light bleaches fluorescence after some minutes simplifying subsequent measurements by removing unwanted light from fluorescence dyes. Spectra of the 29 particles previously investigated are recorded again at this point five times consecutively (Figure 3b shows the resulting resonance wavelength for one particle as a function of experimental time elapsed). To bind streptavidin to the biotinylated membrane, we rinse with a solution containing 1 mg/mL streptavidin in the identical buffer solution and incubate for 20 min. Unbound streptavidin is removed by rinsing for another 20 min with pure buffer, and the particle spectra are measured again. In the next step, we remove the streptavidin layer with protease (protease from *Streptomyces griseus*, Sigma Aldrich: P8811, 2 mg/mL). The protease causes a white precipitate and thus an enormous increase of the scattering background making a direct spectral investigation of single nanoparticles impossible. Therefore, we wash with a cleaning solution (Triton x-100, 4% (v/v)) for 10 min to remove the proteins and the membrane and rinse for 10 min with buffer. At this point, the final spectra of the 29 particles monitored in this experiment are measured.

Figure 3a shows the single particle scattering spectra for a typical gold rod used in the experiments. Initially, the particle is immersed in buffer and has a resonance wavelength of  $656.8 \pm 1.4$  nm (the error quoted is the standard deviation from five independent measurements). Spreading the membrane on the substrate over the particles results in a red-shifted resonance at  $662.9 \pm 0.9$  nm, a shift of 6.1 nm to the initial value. Addition of streptavidin to the system further increases the resonance wavelength to  $665.4 \pm 0.3$  nm, that is, an additional shift of 2.5 nm, presumably due to a layer of streptavidin on the membrane. Removing the streptavidin and the membrane by protease and Triton x-100 shifts the spectrum back to  $658.6 \pm 0.9$  nm, only 1.8 nm higher than the initial resonance wavelength.

The same data as above is available for 29 particles analyzed in parallel during the above experiment. Considering all 29 particles, we observe a median shift of  $3.6 \pm 1.5$  nm due to spreading the membrane and a second shift of

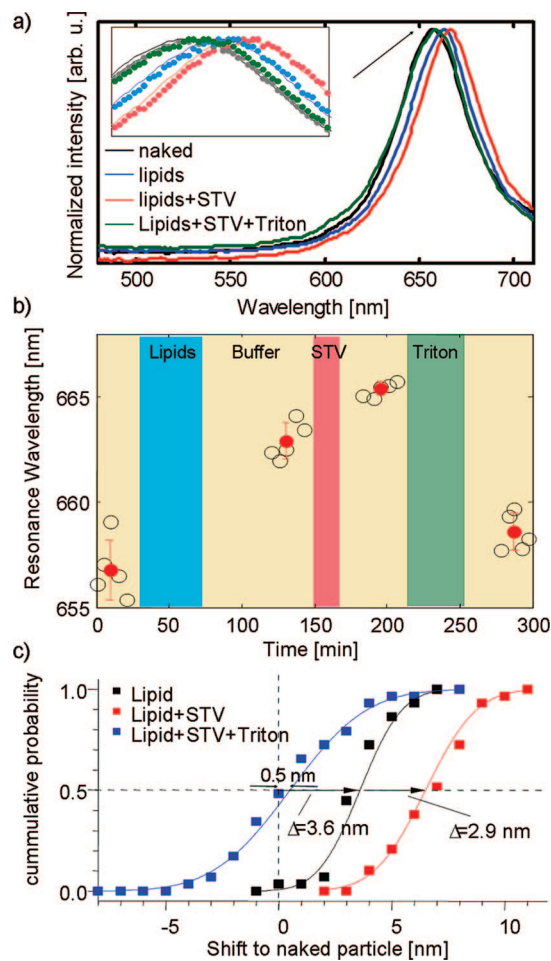


**Figure 3.** (a) Measured scattering spectra for one single particle with different coatings: initially naked, then covered by a biotinylated membrane, followed by a layer of streptavidin, and finally after washing with Triton x-100 to remove the entire membrane coating. The inset shows the raw data (points) and the corresponding smoothed lines. (b) The resonance wavelengths extracted from single particle spectra of one individual particle measured over the course of the experiment (black circles, mean in red with standard deviations). Shadings indicate the experimental steps. (c) Cumulative probability of spectral shifts derived from observing 29 particles parallel to the particle in b. We observe a median shift of  $\Delta_m = 3.6 \pm 1.5$  nm (black dots) after covering the particles with a membrane. Addition of streptavidin leads to a second shift of  $\Delta_s = 2.9 \pm 1.8$  nm. After rinsing with protease and Triton x-100 (to remove the proteins and the membrane), the resonance wavelength is  $\Delta_t = 0.5 \pm 2.7$  nm shifted compared with the beginning of the experiment. The solid lines show the cumulative probability for a Gaussian distribution with the listed median values and standard deviations.

$2.9 \pm 1.8$  nm because of the binding of streptavidin to the membrane. After removing both layers, the resonance wavelength shifts  $0.5 \pm 2.7$  nm compared with the beginning of the experiment (Figure 3c). Repeated experiments under similar conditions show shifts due to spreading of the membrane between 3.5 and 5.4 nm (Supporting Information, Figure S3 and S4), depending on lipid concentration and incubation time. Furthermore, we perform a control experiment with lipids containing no biotin. Here, the incubation with streptavidin results in a negligible shift of  $0.6 \pm 1.8$  nm (Figure S4, Supporting Information). This small shift may

be a sign that not all rods are completely membrane covered<sup>12</sup> and streptavidin attaches nonspecifically to their surface. Wrapping of particles as envisioned in Figure 1a is governed by the interplay of membrane adhesion to both the particle and the glass surface with curvature energy required to bend the membrane at the boundary. The exact shape of the membrane is therefore a function of adhesion energy, particle size, and phospholipid structure.

In order to compare our experimental findings with theory, we estimate the plasmon shifts using the quasi-static approximation for rods with spherical shaped endcaps.<sup>18,19</sup> This theory neglects the effects of particle volume and glass substrate. Within this quasi-static approximation, a “naked” rod of  $56 \times 26$  nm size and immersed in water has a resonance wavelength of 622.1 nm. For the same particle surrounded by a shell corresponding to the membrane thickness (3.95 nm) with a refractive index of  $n = 1.5$ , the resonance wavelength shifts by 15.2 nm. Increasing the shell-thickness to 6.29 nm (3.95 nm thickness of the membrane plus 2.34 nm for streptavidin) leads to a second shift of 5.8 nm (Supporting Information, Figure S5). The theoretically predicted shifts are therefore two to four times larger than the experimental results. Since the calculations above assume a completely coated rod, but in the experiments the rods touch the membrane only on one side (Figure 1), a smaller shift in the experiment is reasonable. Another reason for the smaller measured shift can be a result of defects in the membrane where the rod is not entirely covered.

Furthermore, we test whether the sensitivity of the plasmon shift is sufficient to determine the influence of a small spacer connecting the biotin to the lipid headgroup. For this purpose, three identical experiments as described above are performed with the only difference being the composition of the lipids: (I) with biotin directly connected to the lipid headgroup (Biotin-DHPE), (II) with biotin attached via a short C<sub>6</sub> spacer (Biotin-X-DHPE), and (III) a control experiment with no biotin at all. Figure 4 shows the cumulative probabilities for finding plasmon shifts in the three cases. The median shift due to attaching streptavidin is  $5.3 \pm 3.1$  nm for the membrane containing biotin without a spacer,  $2.4 \pm 2.1$  nm for the membrane with a spacer between the membrane and the biotin, and only  $1.2 \pm 1.0$  nm for the membrane without any biotin. Attaching the streptavidin to the membrane via a short linker results therefore in a smaller spectral shift due to the increased separation compared with the direct linking. This can be explained by the well-known decay in plasmon sensitivity with distance from the nanoparticle surface (Supporting Information, Figure S6).

Membrane coated plasmonic nanoparticles provide a sensing platform that combines single particle sensing with a perfectly functionalized native coating. In this way, nanoparticles can serve as reporters for cellular reactions taking place on and within biological membranes. Lateral heterogeneity of cellular membranes can be probed with nanometer resolution employing monoclonal antibodies to detect small lipid domains or protein clusters on the membrane surface. Furthermore, membrane coated particles offer the advantage to suppress unwanted nonspecific

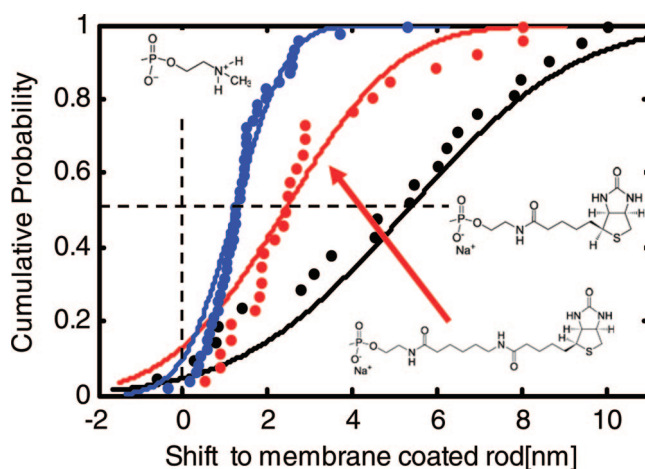


**Figure 4.** Cumulative probability of the spectral shifts due to attachment of streptavidin to gold nanorods coated with different lipids. Attaching streptavidin to rods coated with lipids including biotin leads to a shift of  $\Delta_s = 5.3 \pm 3.1$  nm (block dots). By using lipids, instead, with biotin including a spacer, the spectral shift is smaller and results in  $\Delta_s = 2.4 \pm 2.1$  nm (red dots). A lipid without any biotin leads to a small shift of  $\Delta_s = 1.2 \pm 1.0$  nm due to a nonspecific binding to the gold rod surface. The solid lines show the cumulative probability for a Gaussian distribution with the listed median values and standard deviations.

interactions because of the presence of the membrane, while providing an extremely small active area. Hence, it will be conceivable to create sensors based on the detection of equilibrium coverage fluctuations that would circumvent problems arising from mass transport and drift of the sensor signal. As a consequence, complex processes such as cooperative adsorption, adsorption to heterogeneous surfaces, and slowly evolving systems can be addressed by fluctuation analysis.

**Acknowledgment.** C.S. acknowledges financial support by the Deutsche Forschungsgemeinschaft (DFG) through an Emmy Noether Research Grant. A.J. thanks the DFG (JA 963/6-2) for financial support. J.B. was supported by the Carl-Zeiss-Stiftung.

**Supporting Information Available:** Detailed experimental methods, FRAP experiments proving fluidity of the membrane (Figure S1), Streptavidin-membrane interaction followed by ellipsometry (Figure S2), an additional single particle binding experiment (Figure S3), control experiment on nonbiotinylated membranes (Figure S4), calculated plasmon spectra of membrane coated rods (Figure S5 and S6). This material is available free of charge via the Internet at <http://pubs.acs.org>.

## References

- (1) Lüthgens, E.; Janshoff, A. *ChemPhysChem* **2005**, *6*, 444–448.
- (2) Sönnichsen, C.; Geier, S.; Hecker, N. E.; von Plessen, G.; Feldmann, J.; Ditzbacher, H.; Lamprecht, B.; Krenn, J. R.; Aussenegg, F. R.; Chan, V. Z. H.; Spatz, J. P.; Möller, M. *Appl. Phys. Lett.* **2000**, *77*, 2949–2951.
- (3) Raschke, G.; Kowarik, S.; Franzl, T.; Sönnichsen, C.; Klar, T. A.; Feldmann, J.; Nichtl, A.; Kurzinger, K. *Nano Lett.* **2003**, *3*, 935–938.
- (4) Nusz, G. J.; Marinakos, S. M.; Curry, A. C.; Dahlin, A.; Hook, F.; Wax, A.; Chilkoti, A. *Anal. Chem.* **2008**, *80*, 984–989.
- (5) McFarland, A. D.; Van Duyne, R. P. *Nano Lett.* **2003**, *3*, 1057–1062.

- (6) Rajendran, L.; Simons, K. J. *Cell Sci.* **2005**, *118*, 1099–1102.
- (7) Yethiraj, A.; Weisshaar, J. C. *Biophys. J.* **2007**, *93*, 3113–3119.
- (8) Janshoff, A.; Steinem, C. *Anal. Bioanal. Chem.* **2006**, *385*, 433–451.
- (9) Tanaka, M.; Sackmann, E. *Nature* **2005**, *437*, 656–663.
- (10) Schmitt, E. K.; Nurnabi, M.; Bushby, R. J.; Steinem, C. *Soft Matter* **2008**, *4*, 250–253.
- (11) Mornet, S.; Lambert, O.; Duguet, E.; Brisson, A. *Nano Lett.* **2005**, *5*, 281–285.
- (12) Roiter Y.; Ornatska M.; Rammohan A. R.; Balakrishnan J.; Heine D. R.; Minko, S. *Nano Lett.* **2008**, *8*, 941–944.
- (13) Mayer, L. D.; Hope, M. J.; Cullis, P. R. *Biochim. Biophys. Acta* **1986**, *858*, 161–168.
- (14) Benda, A.; Benes, M.; Marecek, V.; Lhotsky, A.; Hermens, W. T.; Hof, M. *Langmuir* **2003**, *19*, 4120–4126.
- (15) Nikoobakht, B.; El-Sayed, M. A. *Chem. Mater.* **2003**, *15*, 1957–1962.
- (16) Becker, J.; Schubert, O.; Sönnichsen, C. *Nano Lett.* **2007**, *7*, 1664–1669.
- (17) Sönnichsen, C.; Franzl, T.; Wilk, T.; von Plessen, G.; Feldmann, J.; Wilson, O.; Mulvaney, P. *Phys. Rev. Lett.* **2002**, *88*, 077402.
- (18) Liu, M. Z.; Guyot-Sionnest, P. *J. Phys. Chem. B* **2004**, *108*, 5882–5888.
- (19) Prescott, S. W.; Mulvaney, P. *J. Appl. Phys.* **2006**, *99*.
- (20) Janshoff, A.; Kunneke, S. *Eur. Biophys. J. Biophys. Lett.* **2000**, *29*, 549–554.

NL080805L